Electrical transport properties of $LaNi_{1-x}M_xO_3$ (M = Co, Mn) thin films fabricated by pulsed laser deposition

2005 J. Phys.: Condens. Matter 17 6445

(http://iopscience.iop.org/0953-8984/17/41/015)

INSTITUTE OF PHYSICS PUBLISHING JOURNAL OF PHYSICS: CONDENSED MATTER

J. Phys.: Condens. Matter **17** (2005) 6445–6458 doi:10.1088/0953-8984/17/41/015

Electrical transport properties of $LaNi_{1-x}M_xO_3$ (M = Co, Mn) thin films fabricated by pulsed laser deposition

I Chaitanya Lekshmi[1], **Arup Gayen and M S Hegde**

Solid State and Structural Chemistry Unit, Indian Institute of Science, Bangalore, 560 012, India

E-mail: ic.lekshmi@gmail.com, arup@sscu.iisc.ernet.in and mshegde@sscu.iisc.ernet.in

Received 12 March 2005, in final form 31 August 2005
Published 30 September 2005
Online at stacks.iop.org/JPhysCM/17/6445

Abstract

Highly oriented thin films of $LaNi_{1-x}M_xO_3$ (M = Mn, Co) are grown on $LaAlO_3$(100) substrate by pulsed laser deposition. They undergo a metal to insulator transition when the Mn or Co concentration is increased. The observed conduction pattern is highly sensitive to the doping concentration in these thin films. The conduction pattern also varies as the doping element is varied from Mn to Co. There is a large dominance of electron–lattice interactions in the conduction mechanism of the charge carriers. While the metallic thin films of $LaNi_{1-x}Co_xO_3$ show a linear variation of resistivity with temperature, $LaNi_{1-x}Mn_xO_3$ thin films exhibit a prominent square-root dependence of resistivity on temperature. At high concentrations of Mn or Co, the conduction takes place via a polaron hopping mechanism, which suggests that lattice polarization may be present in these films. The change observed in the transport properties is attributed to the charge disproportionation between the Ni^{3+}–Ni^{2+} pairs, which are favoured more in Mn doped thin films. The photoelectron spectroscopic studies give evidence of charge disproportionation present in these films.

1. Introduction

The electrical behaviour of perovskite oxides is largely explained in terms of transition from localized to collective electron states and is often interpreted based on conduction models implying hopping activation of charge carriers and electron–electron interactions when the system changes from an insulator to a metal [1–5]. These transitions can be temperature or structure driven [6, 7] or can be affected by the application of the pressure [8, 9], but in a large number of materials they are often caused by a change in the composition [2, 10–14]. The chemical substitution in transition metal perovskite oxides often results in the mixed valency

[1] Author to whom any correspondence should be addressed.

of the transition metal cations which leads to interesting electronic, magnetic and structural changes.

Perovskite oxides having nickel ions in the B site of the lattice are comparatively less studied, mainly due to the difficulty in stabilizing mixed oxides of Ni in two different oxidation states. When Ni cations are present in mixed-valent state, electrical and magnetic properties can be qualitatively related to the relative numbers of Ni^{2+} and Ni^{3+} cations present, taking into account the possible antiferromagnetic or ferromagnetic interactions and the evolution of electronic localization in the system [1, 15]. Both structural aspects and electronic correlation effects seem to be responsible for much of the observed behaviour in these materials.

$LaNi_{1-x}Mn_xO_3$ and $LaNi_{1-x}Co_xO_3$ systems are known for their interesting magnetic and magnetoresistance properties at low temperatures [16–20]. Goodenough *et al* have reported that ternary oxides $LaM_{1-x}Mn_xO_3$ (M = Ni, Co) are ferromagnets [21]. The ferromagnetism in these compounds is governed by the positive super-exchange interaction between Ni^{2+} (or Co^{2+}) and Mn^{4+} ions via oxygen anions as suggested by Blasse [22]. Spectroscopic studies on $LaMn_{1-x}Co_xO_3$ have shown the presence of both Mn^{3+} and Mn^{4+} species and the observed ferromagnetism in this compound is accounted for by the double-exchange mechanism [23]. Conflicting views exists in the case of $LaNi_{1-x}Mn_xO_3$ compounds regarding their electronic configuration. While compounds prepared by high temperature solid state methods [22, 24, 25] are reported to have Mn^{4+} and Ni^{2+} ionic species present in them, those prepared by low temperature precursor routes [19] have Mn^{3+} and Ni^{3+} ions. Neutron diffraction studies suggest an ordered arrangement of Ni and Mn atoms in $LaNi_{0.5}Mn_{0.5}O_3$ compound, but a random Ni/Mn distribution is deduced for the rest of the series [26]. Sanchez *et al* have shown by x-ray absorption spectroscopic studies that the formal oxidation state of Mn changes continuously from 3+ to 4+ in $LaNi_{1-x}Mn_xO_3$ as the concentration of Mn is increased [27]. A corresponding reduction in Ni valence from Ni^{3+} to Ni^{2+} is observed. Perez *et al* has suggested that the ferromagnetic interaction in $RNi_{0.3}Co_{0.7}O_3$ (where R is a rare earth) is aided by the electron transfer between Ni^{3+} and Co^{3+} ions [18]. However, Park *et al* has shown that Co exists in divalent state in $LaMn_{1-x}Co_xO_3$ [28], which induces Mn^{3+}–Mn^{4+} mixed valence states.

The change in nickel valence is expected to affect the strength of Ni–O–Ni interactions in their oxides. Nickelates being charge-transfer insulators, any change in the metal–ligand interaction should affect the electronic property of the compound. The changes in the NiO_6 octahedra as a result of any alteration in the bond lengths make the role of electron lattice coupling in the conduction mechanism significant. Although these interactions are expected to be more significant in insulators than in metals, nickelates form a special case as they lie in the boundary separating the two regimes.

Selected members of these compounds have been grown in the form of thin films by various deposition techniques including those of pulsed laser deposition [29–32]. But to the best of our knowledge there has been no report of any comprehensive study on the electrical properties of these compounds in the form of thin films over a wide range of composition. The changes in the valence states of the transition metals affect the electrical transport properties and conduction mechanism significantly. We have, in this study, grown thin films of $LaNi_{1-x}M_xO_3$ (M = Co, Mn) by pulsed laser deposition over a range of dopant concentrations and have tried to understand their electrical conduction mechanism.

2. Experimental details

Thin films of $LaNi_{1-x}M_xO_3$ (M = Mn, Co) were fabricated by pulsed laser deposition (PLD) at an oxygen partial pressure of 400 mTorr with an energy density of 2 J cm^{-2} and a repetition

rate of 5 Hz. The energy density was calibrated such that for every pulse a definite thickness of the film was deposited during the ablation. $LaAlO_3$(100) (LAO) was used as the substrate and the substrate temperature was kept at 730 °C. After deposition, the films were cooled to room temperature at an oxygen partial pressure of 140 Torr. For fabricating $LaNiO_3$ thin films the substrate temperature was maintained at 700 °C, the other conditions remaining the same. The films deposited were 3000 Å thick. The targets used for the deposition of $LaNi_{1-x}M_xO_3$ (M = Mn, Co) thin films were prepared by the nitrate method, pelletized and heated at 800 °C for 36 h [33]. The concentration of Mn was varied from $x = 0.05$ to 0.50 and that of Co was varied from $x = 0.10$ to 0.50. $LaNiO_3$ was prepared from lanthanum oxide and nickel oxalate dihydrate by the carbonate method [34]. The compound thus prepared was pelletized and heated at 800 °C for 36 h.

The films were characterized by powder x-ray diffraction (XRD) using Cu Kα radiation and by electrical resistivity (dc) measurements. The electrical resistance measurements were made in the temperature range 10–300 K and for selected samples the resistance was measured up to 4.6 K. The homogeneity of the films was confirmed by energy dispersive analysis of x-ray within the experimental error (2%). The thickness of the films was confirmed using cross-sectional scanning electron microscopy. X-ray photoelectron spectra (XPS) of these films were recorded on an ESCA–3 Mark II spectrometer (VG Scientific Ltd, England) using Al Kα radiation (1486.6 eV) at a pass energy of 50 eV. The binding energies of the elements were calculated with respect to the C(1s) peak at 285 eV and were measured with a precision of ± 0.2 eV. For analysis, the samples were placed in an ultra-high vacuum (UHV) chamber at 10^{-9} Torr that houses the analyser. Prior to mounting, the samples were kept in the preparation chamber at UHV (10^{-9} Torr) for 5 h in order to minimize the adsorbed volatile species on the surface.

3. Result

3.1. Structural studies

Thin films of $LaNi_{1-x}Mn_xO_3$ (LNMO) and $LaNi_{1-x}Co_xO_3$ (LNCO) grow in the (100) direction on LAO substrate. The films grown are crystalline, oriented and of single phase as can be seen from their x-ray diffraction patterns given in figures 1 and 2. A detailed structural study of $LaNiO_3$ (LNO) thin films reported from this laboratory earlier has shown that LNO thin films grow epitaxially in the (100) direction on LAO substrate [35]. The out-of-plane lattice parameter (a_0) value obtained for LNO thin films is 3.817(6) Å which is in good agreement with those reported in the literature [16, 36] for bulk as well as thin films of $LaNiO_3$.

There is a systematic change in the a_0 values of Mn and Co doped thin films on varying the dopant concentration. The a_0 value increases gradually on substituting Mn for Ni. But the substitution of Co for Ni results in the decrease of the out-of-plane lattice parameter values, though the change is negligible. This is expected since $LaCoO_3$ is isostructural with $LaNiO_3$ but has a lower lattice parameter value. The a_0 values for the thin films of LNMO and LNCO are given in table 1.

3.2. Electrical properties

LNO thin films exhibit metallic conductivity in the measured temperature range from 4.6–300 K. The resistivity (ρ) varies from 236 $\mu\Omega$ cm at room temperature to 154 $\mu\Omega$ cm at 4.6 K. The values are comparable to those reported for LNO thin films in the literature [37]. At low temperatures, ρ varies as T^2, suggesting strong electron–electron scattering for the charge carriers. However, above 140 K, the temperature dependence of ρ changes over to $T^{1.5}$.

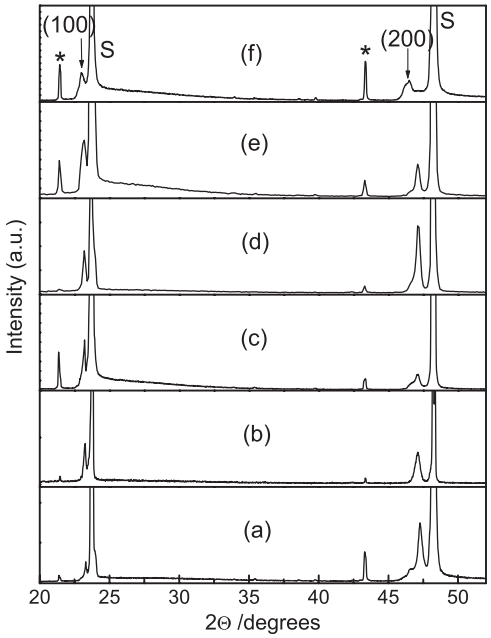

Figure 1. XRD pattern of LNMO thin films on LAO substrate for (a) $x = 0.05$; (b) $x = 0.10$; (c) $x = 0.15$; (d) $x = 0.20$; (e) $x = 0.30$; (f) $x = 0.50$. S denotes the substrate. The * marked peaks correspond to the K_β peaks of the substrate.

Table 1. Out-of-plane lattice parameter values of LNMO and LNCO thin films deposited on LAO(100) substrate.

LNMO		LNCO	
x	a_0 (Å)	x	a_0 (Å)
0.00	3.817(2)	0.00	3.817(2)
0.05	3.818(2)	0.10	3.819(3)
0.10	3.825(3)	0.20	3.819(2)
0.15	3.831(2)	0.25	3.802(2)
0.20	3.834(2)	0.30	3.803(4)
0.25	3.841(3)	0.40	3.792(2)
0.30	3.840(2)	0.50	3.785(3)
0.35	3.856(3)		
0.50	3.867(4)		

Xu *et al* have reported similar temperature dependence in bulk $LaNiO_3$ in the temperature range 100–300 K [38].

On substituting Mn or Co for Ni in the B site of the perovskite lattice, the resistivity of the thin films increases gradually with increasing x. At critical dopant concentrations the films undergo a metal to insulator transition. The variation of resistivity with temperature for various concentrations of Mn and Co respectively in LNMO and LNCO thin films are given in figures 3 and 4. The measurement of ρ versus T for $LaNi_{0.5}Mn_{0.5}O_3$ thin film by the four-probe method could not be made due to its high resistance.

LNCO thin films have positive temperature coefficient of resistivity in the temperature range 10–300 K for low concentrations of Co. At $x = 0.2$, a small upturn in resistivity is observed at low temperatures, below 60 K, indicating the disorder that is induced in the system.

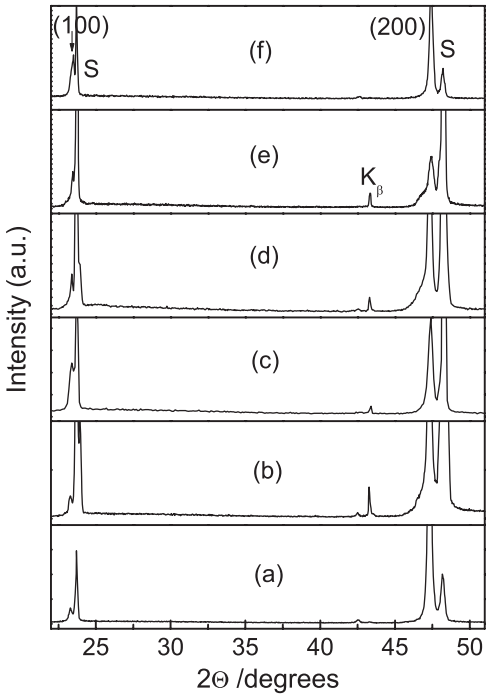

Figure 2. XRD pattern of LNCO thin films on LAO substrate for (a) $x = 0.10$; (b) $x = 0.2$; (c) $x = 0.25$; (d) $x = 0.30$; (e) $x = 0.40$; (f) $x = 0.50$. S denotes the substrate.

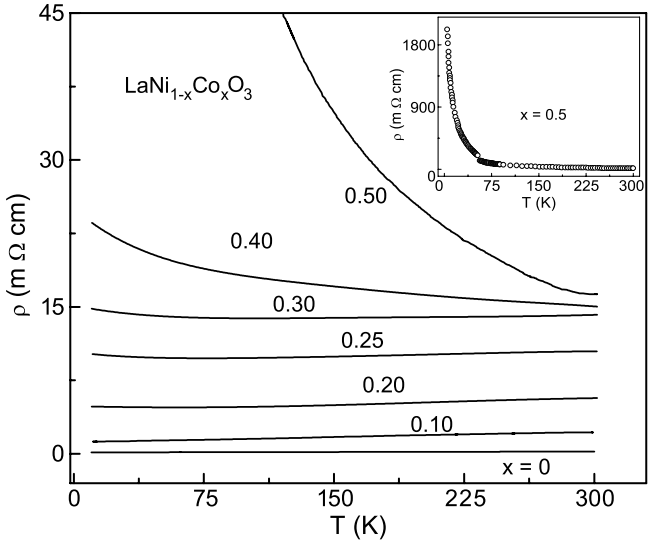

Figure 3. Resistivity versus temperature plots of LNCO thin films on LAO substrate. ρ versus T plot of $x = 0.5$ for the whole temperature range measured is shown in the inset.

Above $x = 0.3$, the resistivity increases gradually with decreasing temperature. When x is raised to 0.5, the rise in resistance on cooling is very rapid as can be seen from figure 3. The whole range of resistivity measurement done for $x = 0.5$ is given in the inset of the figure

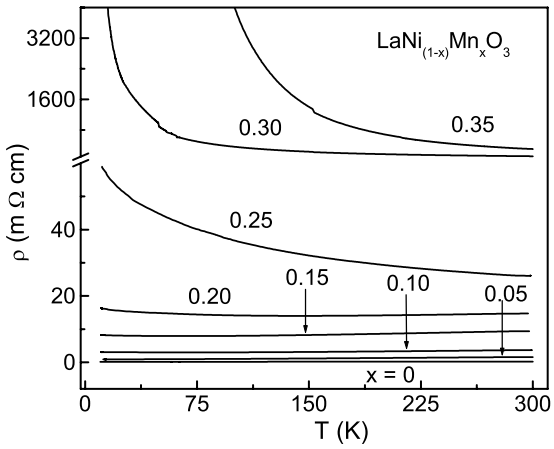

Figure 4. Resistivity versus temperature plots of LNMO thin films on LAO substrate.

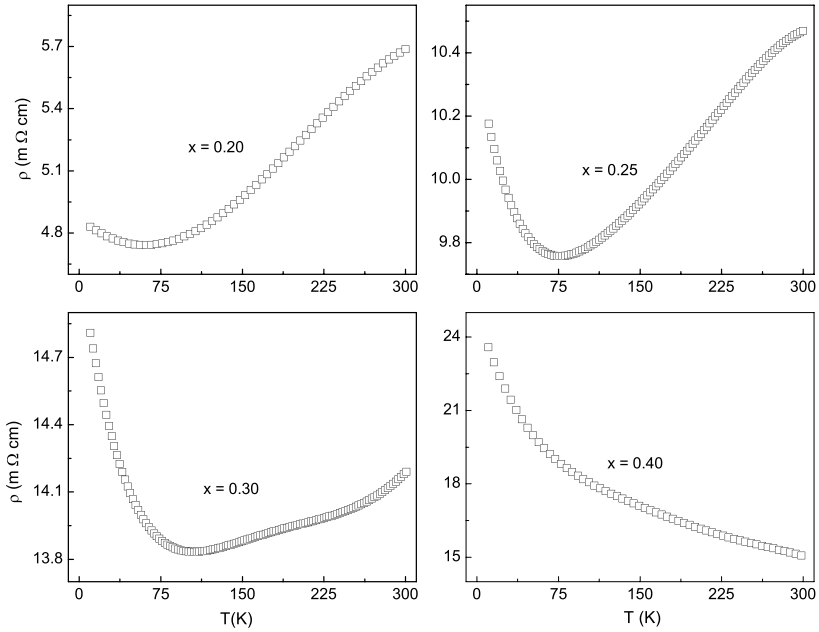

Figure 5. ρ versus T plots of LNCO thin films for $x = 0.20, 0.25, 0.30$ and 0.40 in the temperature range, 10 K $< T <$ 300 K.

for the purpose of clarity. Thus in the composition range $0.2 \leqslant x \leqslant 0.4$ LNCO thin films exhibit transition from metallic to semiconducting behaviour. The temperature dependence of resistivity data for LNCO samples where measurements were made up to 4.6 K, when extrapolated to zero temperature, tend to give finite values for the resistance. As per the scaling theory, LNCO shows insulating behaviour above $x = 0.65$, where $\sigma(0) \rightarrow 0$ is taken as the requirement for the insulating behaviour [39]. However, in our study, we have taken into consideration mainly the change in the temperature coefficient of resistivity in order to determine the transition from metallic to insulating nature. The individual plots of ρ versus T for LNCO thin films in the transition region are given in figure 5. It can be seen that the change

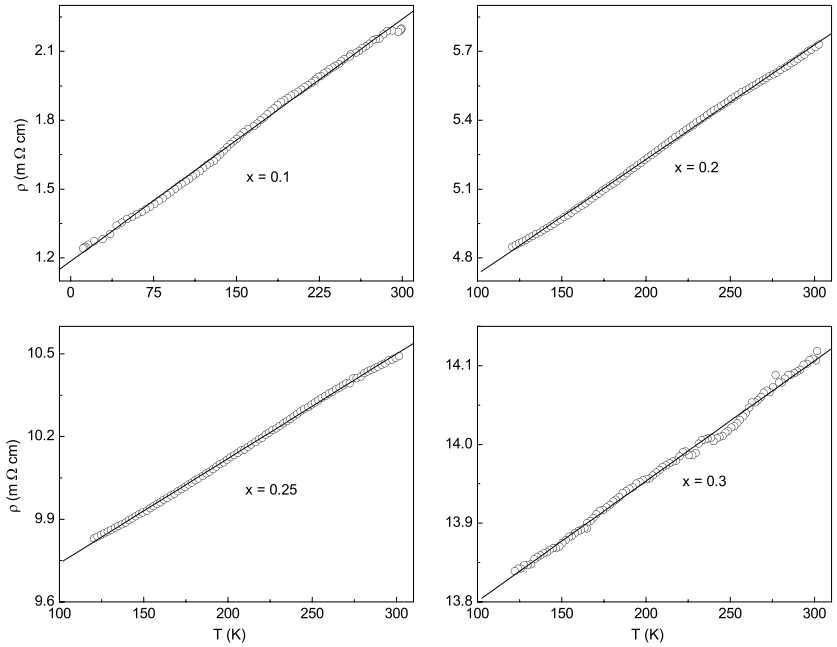

Figure 6. Linear variation of ρ with temperature in LNCO thin films for compositions $x = 0.10$, 0.20, 0.25 and 0.30. The dots represent the observed data and the lines show the linear fitting.

in resistivity is very small ($\leqslant$1 mΩ cm) over the temperature range shown (10 K $< T <$ 300 K) for $x = 0.20$, 0.25 and 0.30. In the metallic regime, LNCO thin films show linear dependence of resistivity on temperature in the region where the temperature coefficient of resistivity is positive (see figure 6).

Among LNMO thin films deposited, a positive temperature coefficient for resistivity over the temperature range 10–300 K is observed for $x = 0.05$. Compared to LNCO thin films, significant deviation is observed for higher Mn doping even above 100 K, as can be seen from figure 7. The transition from metallic to semiconducting behaviour is observed in the composition region $0.10 \leqslant x \leqslant 0.25$. ρ versus T plots of LNMO thin films in the transition region are given in figure 8. Above $x = 0.25$, a drastic increase in resistivity (almost fivefold) is observed and the change of ρ with temperature becomes rapid. However, a non-linear ($T^{1.5}$) dependence of resistivity on temperature is clearly observed in the temperature region 140–300 K for all metallic samples (see figure 9). We have checked the T^2 dependence of resistivity at low temperatures but the dependence observed was not satisfactory.

The variation of room temperature resistivity with concentration for LNCO and LNMO thin films is given in figure 10. LNMO thin films show a slow increase in the room temperature resistivity (ρ_{RT}) till Mn concentration reaches 25%. Beyond that, there is a drastic change in the ρ_{RT} value. On the other hand, the overall change in the room temperature resistivity of LNCO thin films in the composition region $0 < x \leqslant 0.50$ is very small.

On the insulating side of the metal–insulator transition, the conduction of the charge carriers, both in LNMO and LNCO thin films, follows activated behaviour at high temperatures (figure 11). Above 200 K, ρ versus T data can be fitted with the expression for adiabatic small polaron conduction mechanisms (figure 11(a)) given by

$$\rho(T) = \rho_0 T \exp(E_a/k_B T) \tag{1}$$

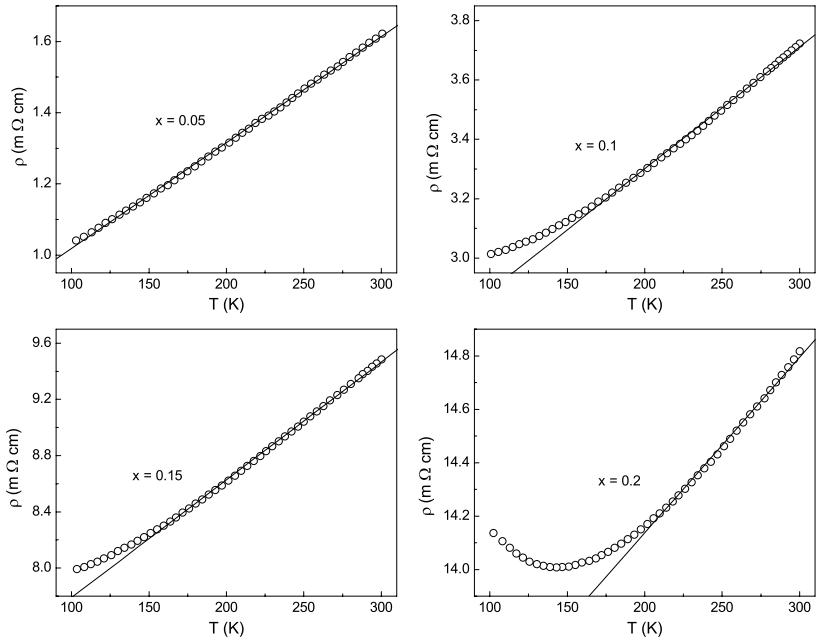

Figure 7. Linear dependence of resistivity on temperature in LNMO thin films for $0.05 \leqslant x \leqslant 0.2$. The dots represent the observed data and the lines show the linear fitting.

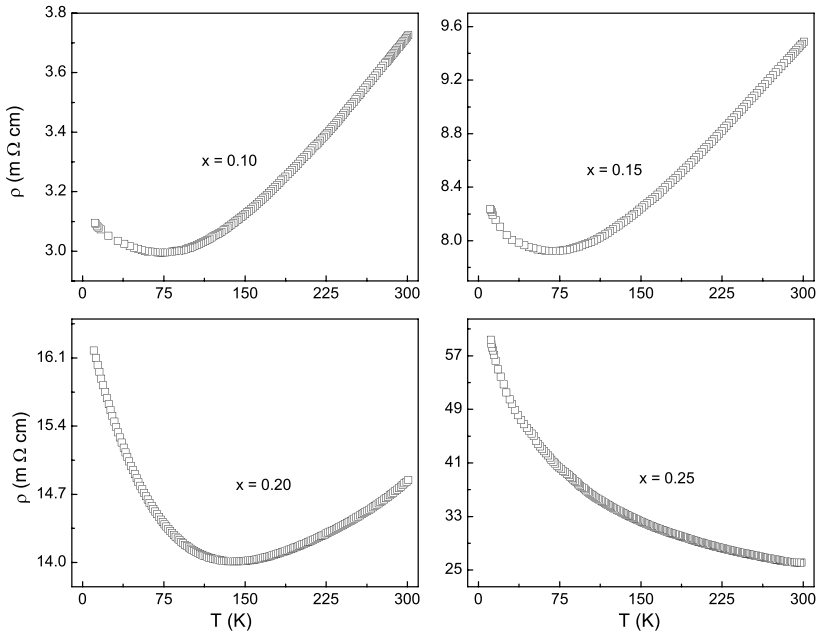

Figure 8. ρ versus T plots of LNMO thin films for $x = 0.10, 0.15, 0.20$ and 0.25 in the temperature region 10 K $< T <$ 300 K.

where E_a is the hopping energy of the small polarons. The values obtained for the hopping energy for each of these films are given in table 2. The small polaron binding energy is directly

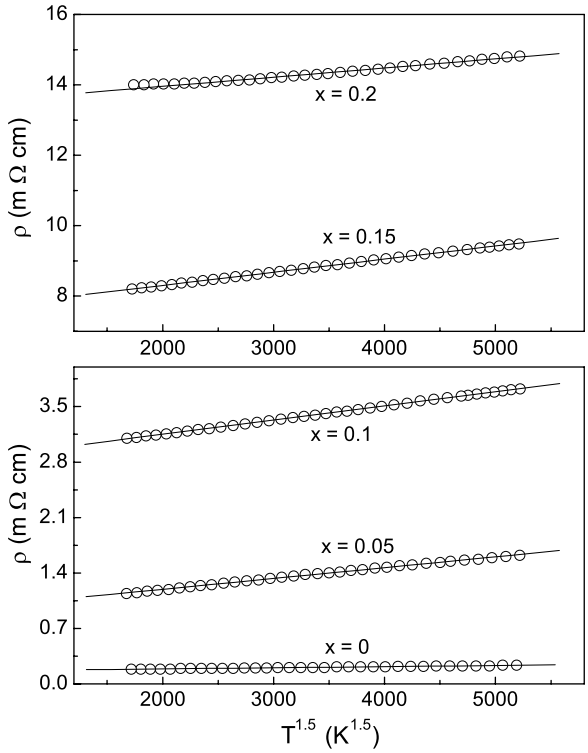

Figure 9. ρ versus $T^{1.5}$ plots of LNMO thin films in the composition range $0 \leqslant x \leqslant 0.20$. The dots represent the observed data and the lines show the linear fitting.

proportional to the hopping energy required. The hopping energy required for the charge carrier conduction depends to a large extent on the distortion present in the films. The tolerance factor of the perovskite (ABO_3) oxide given by the expression $t = (r_A + r_O)/\sqrt{2}(r_B + r_O)$, where r_A, r_B and r_O are respectively the radii of ions A, B and O, is a measure of the distortion present in the system. $LaNiO_3$ has a tolerance factor of 1.0, which facilitates the delocalization of the charge carriers, enhancing the bandwidth. On substituting Mn or Co for Ni, the tolerance factor decreases, the reduction being greater in the case of Mn substitution than for Co. For 35% doping by Mn in $LaNiO_3$, the tolerance factor reduces to 0.988 while 50% doping by Co changes t from 1.0 to 0.99. The perovskite structure accommodates the reduction in tolerance factor by cooperative rotations of MO_6 octahedra, resulting in the buckling of M–O–M bond angle. For large distortion from the ideal cubic structure the electron–lattice interaction increases, which localizes the charge carriers, resulting in higher polaron binding energy [40]. From the table, it is evident that the hopping energy required for conduction is higher in LNMO thin films than in Co doped samples. The high temperature region of the resistivity data in these films also fits well with the Arrhenius activation mechanism (figure 11(b)) given by

$$\rho(T) = \rho_0 \exp(E_b/k_B T) \tag{2}$$

where E_b gives the corresponding activation energy.

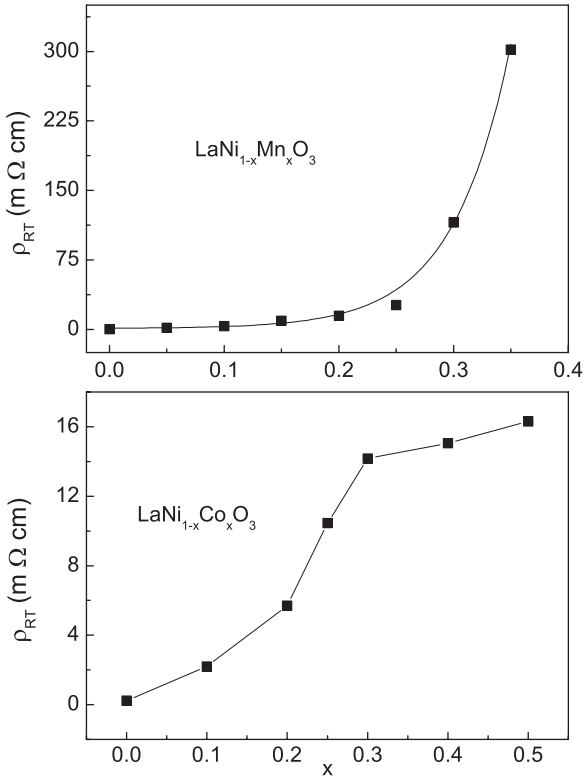

Figure 10. Plot of room temperature resistivity versus concentration for LNMO and LNCO thin films. The lines through the data points are guides to the eye.

Table 2. The activation energies obtained for LNMO and LNCO thin films by fitting the temperature dependence of resistivity data to the adiabatic small polaron hopping as well as to the Arrhenius activation mechanisms. E_a corresponds to the small polaron hopping energy and E_b corresponds to the activation energy by Arrhenius activation.

LNMO			LNCO		
x	E_a (meV)	E_b (meV)	x	E_a (meV)	E_b (meV)
0.35	64.4	42.7	0.50	52.2	30.1
0.30	42.8	20.9	0.40	30.6	8.8
0.25	28.0	6.6			

3.3. XPS studies

XPS core level spectra of $LaNi_{0.65}Mn_{0.35}O_3$, $LaNi_{0.5}Mn_{0.5}O_3$, $LaNi_{0.5}Co_{0.5}O_3$ and $LaNiO_3$ thin films are recorded. There are contradictory reports about the possible oxidation states of Ni, Mn and Co at which these compounds stabilize. It is important to know the oxidation states of the above transition metals in order to understand the transport properties exhibited. Figure 12 gives the XPS core level spectra of La(3d) + Ni(2p) region in LNMO, LNCO and LNO thin films.

La(3d) + Ni(2p) core level regions extending from 820 to 880 eV in LNMO, LNCO and LNO thin films are compared with those of $LiNiO_2$ bulk solid (synthesized in our laboratory)

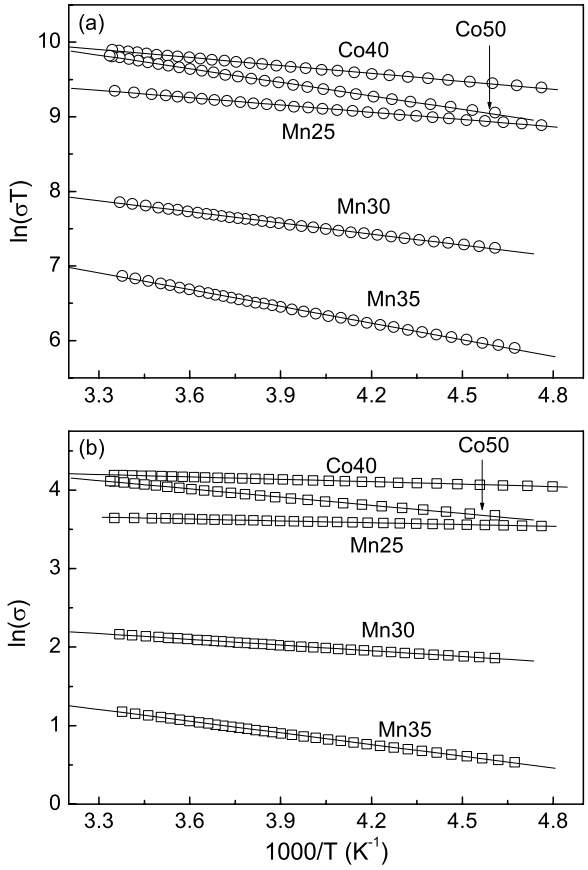

Figure 11. (a) ln σT versus $1000/T$; (b) ln σ versus $1000/T$ plots of LNCO ($x = 0.4$, 0.5) and LNMO ($x = 0.25$, 0.3, 0.35) thin films. The dots represent the observed data and the lines show the linear fitting.

as well as with those of bulk La_2O_3. The peaks corresponding to La(3d) core level spectra in these films match well with the corresponding peaks in bulk La_2O_3. However, the ratio of intensities of the peak at 851 eV to that at 855 eV decreases in all the films studied compared to that of La_2O_3, indicating the presence of Ni 2p in this spectral region.

On adding Mn in LNMO thin films, the peak around 855 eV broadens and the peak position shifts slightly to the left, indicating the reduction in nickel valence state. The position of the new peak is in close agreement with that expected for Ni^{2+} in NiO. The intensity of this low binding energy peak increases as the Mn concentration is increased and the feature becomes sharp. The changes observed in the La(3d) + Ni(2p) spectral region are less prominent for $LaNi_{0.5}Co_{0.5}O_3$ thin film compared to those of $LaNi_{0.5}Mn_{0.5}O_3$ thin film. From the above spectra it can be concluded that on substituting Mn or Co for Ni in $LaNiO_3$ a reduction in the oxidation state of Ni takes place. The corresponding changes in the Mn(2p) and Co(2p) spectra could not be studied since the signals were weak.

4. Discussion

$LaNiO_3$ is located very close to the boundary separating 'low-Δ metals' from charge-transfer insulators. The electrical conduction is caused by the correlated motion of charge carriers in the narrow conduction band formed by the electrons of the transition metal [41]. The substitution of Ni by Mn or Co introduces disorder into the system which can significantly

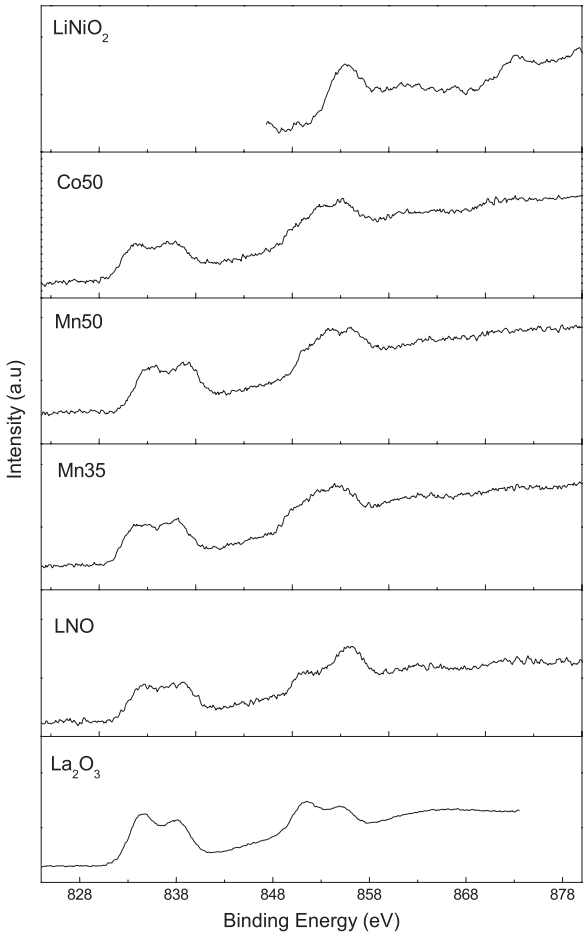

Figure 12. La(3d) + Ni(2p) core level spectra of LNMO, LNCO and LNO thin films. Mn35, Mn50 and Co50 correspond respectively to $LaNi_{0.65}Mn_{0.35}O_3$, $LaNi_{0.5}Mn_{0.5}O_3$ and $LaNi_{0.5}Co_{0.5}O_3$ thin films.

affect the correlated motion. In general, the electrical behaviour can be explained in terms of localized to collective electron transitions and can be interpreted on the basis of conduction models implying hopping activation of charge carriers.

The T^2 dependence of resistivity observed at low temperatures in $LaNiO_3$ thin films changes over to $T^{1.5}$ dependence at higher temperatures. LNMO thin films also exhibit $T^{1.5}$ dependence at low concentrations of manganese. The non-linear dependence observed can be an artifact of the co-existence of electron–electron and electron–phonon interactions [42]. However, the T^2 dependence observed at low temperatures in LNMO thin films is not satisfactory. So it is difficult to point out explicitly the origin of the $T^{1.5}$ dependence observed from our study. The effect of substitution is clearly seen above $x = 0.05$ in LNMO thin films as we observe an upturn in the temperature dependence of resistivity at low temperatures. At higher temperatures the entropic factors allow better overlapping of the orbitals, giving rise to metallic conduction [1, 15]. A charge transfer gap appears in these nickelate thin films as the doping is further increased, leading to greater localization of the charge carriers [1, 15]. The electronic localization in perovskite oxides can be due to static disorder [43] or electron–electron interactions [44–47] leading to square root dependence of resistance at low temperatures or by electron lattice coupling [40, 43, 48]. As the degree of static disorder increases, a metallic conductor transforms into an insulator where the energy

gap separates the metallic extended states from those of localized states. At the same time, nickelates being narrow band compounds, the effects of electron–electron interactions should be strong. It is rather difficult to point to any one of these factors as the cause of the observed temperature dependence of ρ for the films studied here.

When x reaches 0.25, the conduction occurs via a polaron hopping mechanism. Similar results have been reported for related systems [10, 23] and the above mechanism would suggest the presence of electronic localization as a consequence of lattice polarization. XPS studies show the reduction in nickel valence state in LNMO thin films supporting the relation $Ni^{3+} + Mn^{3+} \leftrightarrow Ni^{2+} + Mn^{4+}$. Both Mn^{3+} and Ni^{3+} being Jahn–Teller ions, lattice polarization can be expected. Since the electronic structure of nickelates is strongly dependent on the degree of hybridization between Ni (3d) and O (2p) bands [1], any change in the valence state of these elements will have profound influence on their electrical properties. More precise studies are required to determine the extent of charge disproportionation present in these thin films. The reduction of nickel oxidation state is comparatively less in LNCO thin film. At low concentrations of Co ($x < 0.40$) the charge disproportionation, $Ni^{3+} + Co^{3+} \leftrightarrow Ni^{2+} + Co^{4+}$, present may be negligible. Equation (2) and the activation energy E_b refers to the situation where the interaction of the electron with the phonons is neglected and the states close to the Fermi energy of the charge carriers are localized [40]. However, when the interaction of the charge carriers with lattice vibrations becomes appreciable polaronic transport is considered. A carrier in such cases will have higher effective mass and lower mobility. In order for the carriers to move, the lattice site must distort by means of thermal fluctuations and the energies involved are normally high [49]. This explains the difference in activation energies obtained using equations (1) and (2). We do not know at this point why both the equations are simultaneously satisfied for the films studied.

Though similar conclusions can be drawn for LNCO thin films as that of LNMO thin films regarding the effects of substitution, there are subtle differences in the conduction mechanism between the two sets of thin films. The $T^{1.5}$ dependence of ρ is not observed for LNCO thin films in the temperature range studied here. The variation of resistivity with temperature is rather linear. While Mn doped samples show drastic increase in room temperature resistivity above $x = 0.3$, the variation is gradual and small for LNCO thin films up to $x = 0.50$. Among the large number of perovskite oxides with high electronic conductivity, $LaNi_{1-x}Co_xO_3$ is one of the most promising materials for electrode purposes mainly because of the nearly constant resistance over a wide range of temperatures and dopant concentrations [32, 50]. We have not measured the resistance below 10 K for all the films studied and hence cannot comment on the electron–electron scattering present at very low temperatures.

The present study on LNMO and LNCO thin films focuses on the role of lattice polarization in localizing the charge carriers. When mixed valency is possible on the B site cation of the perovskite lattice, any chemical substitution at the same site often brings in charge disproportionation between the participating cations. The resulting disorder changes their conduction mechanism significantly and the system often goes through collective to localized electron transitions. The differences observed in the nature of the conduction pattern between Mn and Co doped thin films may be a consequence of the extent of charge disproportionation taking place in them.

Acknowledgment

The authors gratefully acknowledge the financial assistance from the Department of Science and Technology, Government of India, New Delhi.

References

[1] Sreedhar K, McElfresh M, Perry D, Kim D, Metcalf P and Honig J M 1994 *J. Solid State Chem.* **110** 208
[2] Dougier P and Hagenmuller P 1975 *J. Solid State Chem.* **15** 158
[3] Miyasaka S, Okuda T and Tokura Y 2000 *Phys. Rev. Lett.* **85** 5388
[4] Sreedhar K and Honig J M 1996 *J. Solid State Chem.* **125** 47
[5] Spalek J 1990 *J. Solid State Chem.* **88** 70
[6] Torrance J B, Lacorre P, Asavaroengchai C and Metzger R M 1991 *J. Solid State Chem.* **90** 168
[7] Lacorre P, Torrance J B, Pannetier J, Nazzal A I, Wang P W and Huang T C 1991 *J. Solid State Chem.* **91** 225
[8] Obradors X, Paolius L M, Maple M B, Torrance J B, Nazzal A I, Fontcuberta J and Grandos X 1993 *Phys. Rev.* B **47** 12353
[9] Medarde M, Mesot J, Lacorre P, Rosenkranz S, Fischer P and Gobrecht K 1995 *Phys. Rev.* B **52** 9248
[10] Raychaudhuri A K 1995 *Adv. Phys.* **44** 21
[11] Zhang Z and Greenblatt M 1994 *J. Solid State Chem.* **111** 145
[12] Rao C N R, Prakash O and Ganguly P 1975 *J. Solid State Chem.* **15** 186
[13] Raveau B, Maignan A and Caignart V 1995 *J. Solid State Chem.* **117** 424
[14] Mott N F, Pepper M, Pollitt S, Wallis R H and Adkins C J 1975 *Proc. R. Soc.* A **345** 169
[15] Alvarez I, Martínez J L, Veiga M L and Pico C 1996 *J. Solid State Chem.* **125** 47
[16] Androulakis J, Katsarakis N, Viskadourakis Z and Giapintzakis J 2003 *J. Appl. Phys.* **93** 5484
[17] Hammer D, Wu J and Leighton C 2004 *Phys. Rev.* B **69** 134407
[18] Perez J, Garcia J, Blasco J and Stankiewicz J 1998 *Phys. Rev. Lett.* **80** 2401
[19] Vasanthacharya N Y, Ganguly P, Goodenough J B and Rao C N R 1984 *J. Phys. C: Solid State Phys.* **17** 2745
[20] Joly V L J, Joy P A and Date S K 2002 *Phys. Rev.* B **65** 184416
[21] Goodenough J B, Wold A, Arnott R J and Menyuk N 1961 *Phys. Rev.* **124** 373
[22] Blasse G 1965 *J. Phys. Chem. Solids* **26** 1969
[23] Ritter C, Ibarra M R, Morellon L, Blasco J, Garcia J and De Teresa J M 2000 *J. Phys.: Condens. Matter* **12** 8295
[24] Sonobe M and Kichizo A 1978 *J. Phys. Soc. Japan* **61** 4193
[25] Asai K, Sekizawa H and Iida S 1978 *J. Phys. Soc. Japan* **47** 1054
[26] Blasco J, Sánchez M C, Pérez-Cacho J, García J, Subías G and Campo J 2002 *J. Phys. Chem. Solids* **63** 781
[27] Sánchez M C, García J, Blasco J, Subías G and Pérez-Cacho J 2002 *Phys. Rev.* B **65** 144409
[28] Park J H, Cheong S W and Chen C T 1997 *Phys. Rev.* B **55** 11072
[29] Androulakis J, Klini A, Manousaki A, Violakis G and Giapintzakis J 2004 *Appl. Phys.* A **79** 671
[30] Androulakis J and Giapintzakis J 2004 *Mater. Sci. Eng.* B **109** 217
[31] Kim L D and Kim H G 2001 *Japan. J. Appl. Phys.* **40** 2357
[32] Hrovat M, Katsarakis N, Reichmann K, Bernik S, Kuscer D and Hole J 1996 *Solid State Ion.* **83** 99
[33] Lekshmi I C 2004 *PhD Thesis* Indian Institute of Science, Bangalore p 129
[34] Wold A, Post B and Banks E 1957 *J. Am. Chem. Soc.* **79** 4911
[35] Hegde M S, Satyalakshmi K M, Mallya R M, Rajeswari M and Zhang H 1994 *J. Mater. Res.* **9** 898
[36] Kim S S, Kang T S and Je J H 2002 *Thin Solid Films* **405** 117
[37] Satyalakshmi K M, Mallya R M, Ramanathan K V, Wu X D, Brainard B, Gautier D C, Vasanthacharya N Y and Hegde M S 1993 *Appl. Phys. Lett.* **62** 1233
[38] Xu X Q, Peng J L, Li Z Y, Ju H L and Greene R L 1993 *Phys. Rev.* B **48** 1112
[39] Rajeev K P and Raychaudhuri A K 1992 *Phys. Rev.* B **46** 1309
[40] Mott N F 1990 *Metal–Insulator Transitions* 2nd edn (London: Taylor and Francis) p 59
[41] Rajeev K P, Sivashankar G V and Raychaudhuri A K 1991 *Solid State Commun.* **79** 591
[42] Takagi H, Batlogg B, Kao H L, Kwo J, Cava R J, Krajewski J J and Peck W F Jr 1992 *Phys. Rev. Lett.* **69** 2975
[43] Anderson P W 1958 *Phys. Rev.* **109** 1492
[44] Mott N F 1974 *Metal–Insulator Transitions* (London: Taylor and Francis)
[45] Hubbard J 1963 *Proc. R. Soc.* A **276** 238
[46] Hubbard J 1964 *Proc. R. Soc.* A **277** 237
[47] Hubbard J 1964 *Proc. R. Soc.* A **281** 401
[48] Edward P P and Rao C N R (ed) 1985 *The Metallic and Non-Metallic States of Matter* (London: Taylor and Francis)
[49] Elliot S R 1998 *The Physics and Chemistry of Solids* (Chichester: Wiley) p 513
[50] Trummer B, Fruhwirth O, Reichmann K, Holzinger M, Sine W and Polt P 1999 *J. Eur. Ceram. Soc.* **19** 827